Journal of the Physical Society of Japan
Vol. 63, No. 5, May, 1994, pp. 1976-1985

Anisotropic Optical Spectra of $YAlO_3$ (YAP) Single Crystals in the Vacuum Ultraviolet Region. II. Spectra of Reflectivity

Tetsuhiko TOMIKI, Yoshiiku GANAHA, Tohru SHIKENBARU*, Tomoyoshi FUTEMMA**, Masatada YURI[1,***], Yoshihiro AIURA[1,***], Hirohito FUKUTANI[1], Hiroo KATO[2], Tsuneaki MIYAHARA[2], Akira YONESU[3] and Junkoh TAMASHIRO

Department of Physics, College of Science, University of the Ryukyus, Nishihara, Okinawa 903-01
[1]*Institute of Physics, University of Tsukuba, Tsukuba, Ibaraki 305*
[2]*Photon Factory, National Laboratory for High Energy Physics (KEK), Oho, Tsukuba, Ibaraki 305*
[3]*Department of Electrical Engineering, College of Engineering, University of the Ryukyus, Nishihara, Okinawa 903-01*

(Received December 6, 1993)

Anisotropic reflectivity spectra of $YAlO_3$ single crystals at 297 K measured with the light polarized parallel to each of the *a*, *b* and *c* axes are presented in the range from ~6.5 eV to ~120 eV. A comparison of the reflectivity spectra of $YAlO_3$ with those of Y_2O_3, $Y_3Al_5O_{12}$ and α-Al_2O_3 single crystals reaffirms that the peaks at ~35 eV are mainly associated with the $Y^{3+}4p^6$ and the features beyond ~76 eV with the $Al^{3+}L_{2,3}$. Anisotropic reflectivity spectra at 10 K are shown in the region from ~7 eV to 15 eV. Effective optical dielectric constants calculated by the sum rule including the imaginary part of the dielectric constant up to ~120 eV are seen to saturate at the values corresponding to 98.0% ~ 99.7% of the literature values of the optical dielectric constant.

[anisotropic reflectivity spectra, YAP crystals, vuv region]

§1. Introduction

The advent of large, high quality single crystals of $YAlO_3$ was only when Weber *et al.* found in 1969, contrary to expectations based upon the phase studies at that time, that such single crystals could easily be grown by the Czochralski technique.[1] $YAlO_3$ crystallizes in a slightly distorted perovskite structure with an orthorhombic unit cell and is called yttrium aluminate perovskite (YAP). Optically, it is a negative biaxial crystal. The determination of refractive indices was accomplished by measuring each refractive index for light polarized parallel to the *a*, *b* and *c* crystallographic axes in the wavelength range from 1.06 μm to 0.4046 μm.[2] The absorption spectrum of Ce^{3+} doped single crystals of YAP at 300 K was examined with natural light from 2600 nm to 186 nm:[3] A steeper rise of absorption was suggested at ~6.5 eV, but no absorption tail in the intrinsic region of $YAlO_3$ crystals was revealed. Measurements by natural light in the photon-energy range from 3.5 eV to 14 eV were carried out at 300 K on reflectivity spectra from a natural surface of YAP boule grown by the Czochralski method;[4] a steep rise of the absorption at 7.6 eV ~ 7.7 eV was interpreted as the onset of the instrinsic absorption.

Measurements in the VUV region by light polarized parallel to the *a*, *b* and *c* axes have been made on single crystals of $YAlO_3$ mainly by our group.[5-7] A determination of the

* Present address: Miyako Meteorological Observatory, Hirara, Miyako 906.
** Present address: Okinawa Prefectural Government, Naha 900.
*** Present address: Electrotechnical Laboratory, 1-1-4 Umezono, Tsukuba, Ibaraki 305.

Urbach rule parameters describing photon-energy and thermal dependence of the intrinsic absorption in the tail region of YAP was achieved.[7] An interpretation in the famework of the energy levels of the constituent atoms was attempted on main features of the reflectivity spectra in the region of 6.5 eV to 42 eV.[7] Reference 7 will be referred to as I hereinafter. Accuracy of the measurement in I was evaluated as high as ~15% because of a rather high noise level of the apparatus. Owing to disturbance originating from the short wavelength limit of the monochromator employed, in addition, the reflectivity data were found to be no longer accurate enough for detailed analyses in the region from ~35 eV to ~42 eV: A shoulder or dull peak of the energy loss function was derived from the reflectivity data in the region beyond ~36 eV where a plasmon resonance peak is expected to exist.

Recent improvement of the measurement system remarkably reduced the noise level. We have attempted reflectivity measurements once again on $YAlO_3$ single crystals in the VUV region from ~6.5 eV. Use was made here additionally of another type of monochromator for measurements in the region from 23 eV to 120 eV. This has yielded reflectivity data free from the disturbance seen in I in the region from ~35 eV to ~42 eV and revealed the features originating from the $Al^{3+}L_{2,3}$ levels in the region from ~76 eV to ~120 eV.

Section 2 gives a brief account of experimental procedures. Section 3 describes the reflectivity spectra of YAP at room temperature measured with light polarized parallel to each of the crystallographic axes in the region from ~6.5 eV to ~120 eV. The reflectivity data at 10 K in the energy region to 15 eV are also reported. Section 4 gives detailed descriptions on the Kramers-Kronig analysis of the reflectivity spectra measured over a wide range of photon energies from ~6.5 eV to ~120 eV. Estimate on accuracy of the absolute magnitude of each of the anisotropic spectra is presented by use of the sum rule including the dielectric constant as derived from the reflectivity data by the Kramers-Kronig relations.

§2. Experimental Procedures

Samples of YAP single crystals used are the same as those in I; detailed description of the samples were already given there.

Spectroscopic measurements were carried out with the plane polarized light emitted from the 2.5 GeV positron storage ring at KEK (The National Laboratory for High Energy Physics). The light in the photon-energy range of $6\,\text{eV} \lesssim E \lesssim 45\,\text{eV}$ was monochromatized by a Seya-Namioka type monochromator at Beam Line (BL) 11 C, abbreviated as SNM hereinafter, mounted with a fresh, Au-coated concave grating of 1 m radius with 1200 lines/mm. Here E stands for the photon energy. A spectral slit-width $\Delta\lambda \simeq 3.2$ Å was chosen. The data in the region of $23\,\text{eV} \lesssim E \lesssim 120\,\text{eV}$ were obtained with a constant deviation monochromator at BL-11D, abbreviated as CDM hereinafter. This is mounted with the gratings with 600 lines/mm and with 1200 lines/mm. The former was operated in the region of $23\,\text{eV} \lesssim E \lesssim 90\,\text{eV}$ with a spectral slit width $\Delta E \sim 0.12$ eV at $E \simeq 50$ eV, and the latter in the range of $72\,\text{eV} \lesssim E \lesssim 120$ eV with $\Delta E \sim 0.12_8$ eV at $E \sim 80$ eV.

The data of reflectivity (or absorption) free from the effect of the higher order diffraction lights are obtainable in the region of $2100\,\text{Å} \gtrsim \lambda \gtrsim 1050$ Å by adopting plates of LiF as a transmission filter. Because no practical optical filters are available at present over such a wide range of photon energies as in the present experiment, spectral measurements have been carried out without filters in the region of $E \gtrsim 11.5$ eV. Light in the CDM region has been detected by a nude photomultiplier with CuBe photocathode which has a prominent peak at $E \simeq 120$ eV in the spectral response characteristic. A pair of notches at $E \simeq 39.90$ eV and 41.4_0 eV seen in the spectra of reflectivity (cf. Fig. 1) arises from the photocathode response peak in the third order diffraction. Another weaker pair of notches is noticed on the reflectivity spectra at 59.7 eV and ~62 eV; it is caused by the effect of the photocathode response peak in the second order diffraction.

Our reflectivity (and absorption) measurements have been carried out with the plane polarized light at an incident angle of ~10°. The polarization characteristics has been described by the electric field E of the incident light in vacuum and by the crystallographic

direction in the working surface, *e.g.*, $\langle a\rangle /\!/ E$. The notation $\langle a\rangle /\!/ E$ denotes the incident light in vacuum which has the the vibrating plane of E paralle to the plane ab and the wave normal making an angle of 10° with $\langle b\rangle$. For $\langle b\rangle /\!/ E$ ($\langle c\rangle /\!/ E$), the vibrating plane of E of the incident light is parallel to the plane bc (bc) and the wave normal makes an angle of 10° with $\langle c\rangle$ ($\langle b\rangle$) in vacuum.

Reflectivity data $R(E)$ have been obtained by taking the ratio $I_r(E)/I_o(E)$, here the intensities for incident light $I_o(E)$ and reflected light $I_r(E)$ were determined in sequence by repeated scans of the monochromator over a given photon-energy interval. Because detections of $I_r(E)$ and $I_o(E)$ are made on the radiation from the source-ring at difference time, the resultant data of $R(E)$ may be distorted if $I_o(E)$ differs from the incident light intensity at the time of detection of $I_r(E)$. The distortion can be eliminated to a certain extent by selecting only those data which satisfy the condition

$$\frac{I_o(E)}{I'_o(E)}=\text{const of } E, \tag{1}$$

$I_o(E)$ and $I'_o(E)$ being the incident light intensities just before and after the measurement of $I_r(E)$, respectively. All the data in this paper satisfy the condition (1), whereas no such check of the data was made in I because of a lack of a data processing capability at that time.

To avoid the effect due to disturbance *e.g.*, by stray light in the short wavelength limit region of SNM, this paper deals with the reflectivity spectra composed of the data by SNM in the region up to $E\sim 25$ eV and those by CDM in the region of $25\text{ eV}\lesssim E\lesssim 120\text{ eV}$. The accuracy of the reflectivity data R is estimated by repeated scans as

$$\Delta R/R\lesssim \pm 2.2\%. \tag{2a}$$

The reflectivity data $R(E)$ for $\langle a\rangle /\!/ E$ in the region of $E\gtrsim 76$ eV in Fig. 1 exceptionally show a remarkable scattering of the data points. The accuracy in this region is estimated as

$$\Delta R/R\sim \pm 4.5\%. \tag{2b}$$

Descriptions concerning the correction of the wavelength (photon energy) scale of the monochromators used and others were given in refs. 8–10.

§3. Experimental Results

The reflectivity spectra for $\langle a\rangle /\!/ E$, $\langle b\rangle /\!/ E$ and $\langle c\rangle /\!/ E$ of YAP single crystals at 297 K are shown in Fig. 1. Each frame of Fig. 1 contains the reflectivity data measured in the present experiment (full curve) and those calculated from the refractive indices (broken curve) given by a Sellmeir equation

$$n_j^2=1+\frac{A_j\lambda^2}{\lambda^2-B_j^2}, \tag{3}$$

here, λ is a wavelength in μm unit, and j=a, b and c stand for $\langle a\rangle /\!/ E$, $\langle b\rangle /\!/ E$ and $\langle c\rangle /\!/ E$, respectively. The Sellmeir coefficients A_j and B_j were determined by the least-squares fit to the refractive indices measured in the region of $1.17\text{ eV}\lesssim E\lesssim 3.064\text{ eV}$.[2] They are listed in Table I. The broken curves have been drawn in Fig. 1 up to $E\sim 7$ eV where no refractive index data are available. The spectral dependence of the reflectivities in the region of 6 eV to 7 eV was found to be in agreement with that of the calculated ones.

One may notice by the magnitude of $\sqrt{B_j}$ that the term of electronic vibration alone is taken into account in eq. (3). Thus this equation yields

$$\left.\begin{aligned}\varepsilon_{\infty,a}&=3.7038\\ \varepsilon_{\infty,b}&=3.6717\\ \varepsilon_{\infty,c}&=3.6196\end{aligned}\right\}, \tag{4}$$

here, $\varepsilon_{\infty,j}$ stands for the optical dielectric constant with j=a, b and c.

An important difference between the data in Fig. 1 and those in I, besides reduction of noise in the present data, is manifested by the reflectivity structures peaking at 34.5 ~ 35.0 eV: Their peak is more intense and the ratio of the reflectivity at ~40 eV to that at the peak position is smaller in the present work than in I. This is admittedly due to the reflectivity data by CDM adopted in the region of $E\gtrsim 25$ eV which contain no stray light disturbance peculiar to the short wavelength limit region of SNM, $35\text{ eV}\lesssim E\lesssim 42$ eV (cf. §2). In fact, as will be reported separately, the energy loss

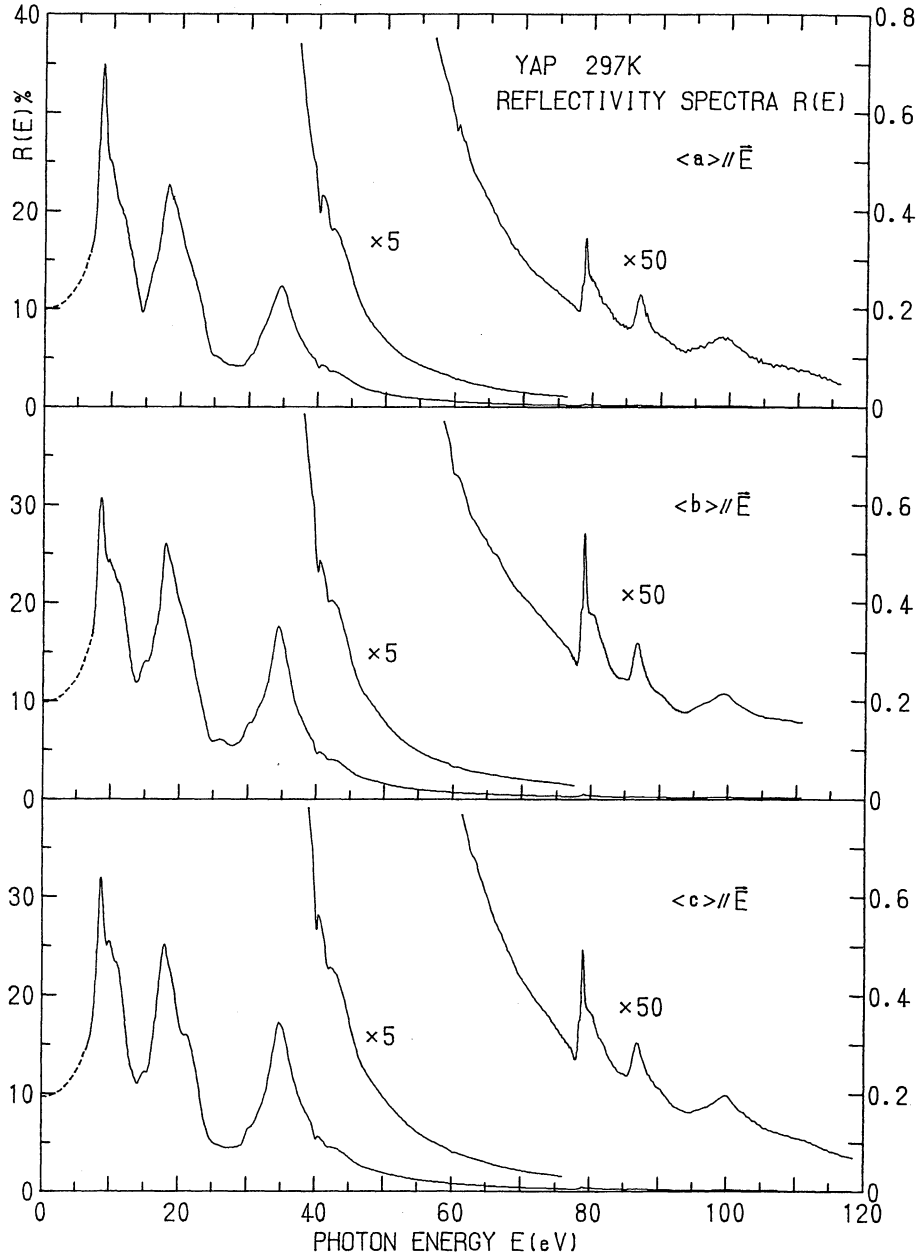

Fig. 1. Reflectivity spectra of YAP single crystals at 297 K measured in the photon-energy range from 6.5 eV to ~120 eV with the light polarized parallel to each of the crystallographic axes. Full curves represent the measured data and broken curves the values calculated from the refractive indices, eq. (3).

functions $-\mathrm{Im}\varepsilon^{-1}$ derived from the spectra in Fig. 1 are of asymmetric bell shape peaking at the plasma resonance position at 36 eV ~ 37 eV. This is very contrasted to a dull peak or shoulder of I in the same region.

Measurements of reflectivity spectra of YAP in the region $E > 42$ eV is made for the first time by the present experiment. Each spectrum in this region consists of a continuum characterized by a monotonic decrease with in-

Table I. Sellmeir coefficients A_j and B_j determined by the dispersion experiment for undoped YAP single crystals;[2] j=a, b and c stand for $\langle a\rangle /\!/$, $\langle b\rangle /\!/$ and $\langle c\rangle /\!/ E$, respectively.

j	a	b	c
A_j	2.70381	2.6717	2.61960
B_j [μm^2]	0.012903	0.012605	0.012338
$\sqrt{B_j}$ [μm]	0.113591	0.112272	0.111077

creasing E and the structure beyond $E\sim 76$ eV superposed on the former.

The reflectivity spectra of single crystals of α-Al_2O_3, Y_2O_3 and thier pseudobinary compounds, YAG ($Y_3Al_5O_{12}$) and YAP, are summarized in Fig. 2. One may notice at once that the prominent reflectivity structures peaking around 34.5 ~ 35.0 eV occur only for the compounds including Y^{3+} as the constituent atom and the reflectivity features in $E\gtrsim 76$ eV only for the compounds including Al^{3+} as the constituent atom. Referring to the energy levels of Y^{3+} free ions,[11] we have interpreted the reflectivity structures peaking around 34.5 eV ~ 35.0 eV as due to the inner core transitions from the $4p^6$ level of Y^{3+} in the single crystals of Y_2O_3, YAP and YAG.[5-7,9,10,12,13] Figure 2 experimentally supports this interpretation. The peak at 32.70 eV in α-Al_2O_3 occupies the position distinct from the Y^{3+}-peak position and probably arises from the interband transitions from $O^{2-}2s^2$- to $Al^{2+}3p$-bands.[14] The reflectivity features in the region $E\gtrsim 76$ eV in the single crystals of α-Al_2O_3 and YAG have been identified with the interband transitions from $Al^{3+}L_{2,3}$ levels[8,10,14,15] in view of the energy levels of Al.[16] Figure 2 confirms that the above interpretation is valid for the optically

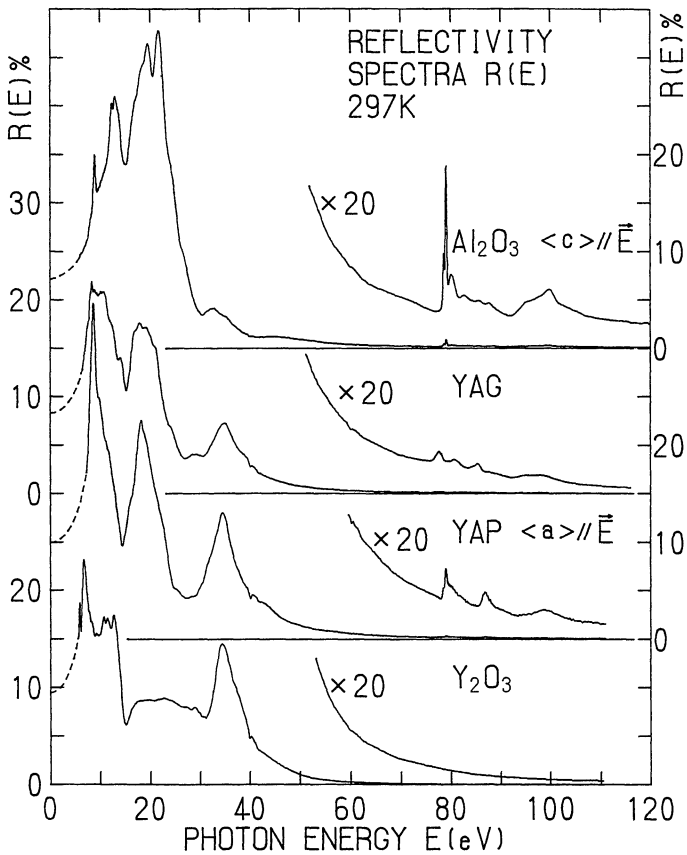

Fig. 2. Reflectivity spectra of single crystals of α-Al_2O_3,[14] Y_2O_3[9] and their pseudobinary compounds, $Y_3Al_5O_{12}$ (YAG)[10] and $YAlO_3$, at 297 K.

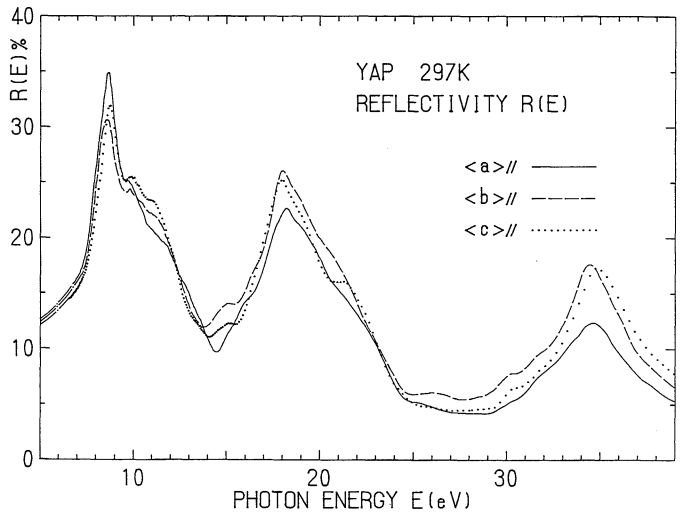

Fig. 3. Reflectivity spectra for $\langle a\rangle // E$ (full curve), $\langle b\rangle // E$ (broken curve) and $\langle c\rangle // E$ (dotted curve) of YAP single crystals at 297 K exhibiting their optical anisotropy and main structures in the range from 5 eV to 39 eV. The chain curves in the region of $E \lesssim 6.5$ eV were calculated from eq. (3).

anisotropic spectra of YAP in the region $E \gtrsim 76$ eV in Fig. 1.

Tables II–IV list the spectral positions of main features in the spectra for $\langle a\rangle //$, $\langle b\rangle //$ and $\langle c\rangle // E$ in Fig. 1, respectively. In order to clearly show an optical anisotropic behavior in the ergion of 5 eV $\lesssim E \lesssim$ 39 eV, the reflectivity spectra for $\langle a\rangle // E$, $\langle b\rangle // E$ and $\langle c\rangle // E$ of YAP at 297 K are plotted in the identical frame over an expanded photon-energy scale in Fig. 3. This may also serve as an illustration for the features listed in Tables II–IV. The shoulder located at ~8.1 eV is most distinctly discernible for $\langle a\rangle // E$ and feebly for $\langle c\rangle // E$. This tendency is the same as that noticed in I. A tentative interpretation on the structures peaking at 8.6 eV ~ 8.7 eV and 18 ~ 18.2 eV as well as on the shoulders stated above have been given in I.

The reflectivity spectra measured at 297 K (open circles) and 10 K (dots) are shown for $\langle a\rangle //$, $\langle b\rangle //$ and $\langle c\rangle // E$ in the photon-energy region from 5 eV to 15 eV in Fig. 4. The dots for $\langle a\rangle // E$, data at 10 K, show a shift of the main peak from 8.65 eV to 8.810 eV revealing more clearly the shoulder at 8.12 eV. The spectrum for $\langle b\rangle // E$ has a flat top from 8.52 eV to 8.65 eV at 297 K which shifts in the region of 8.5 eV ~ 8.8 eV at 10 K suggesting a doublet

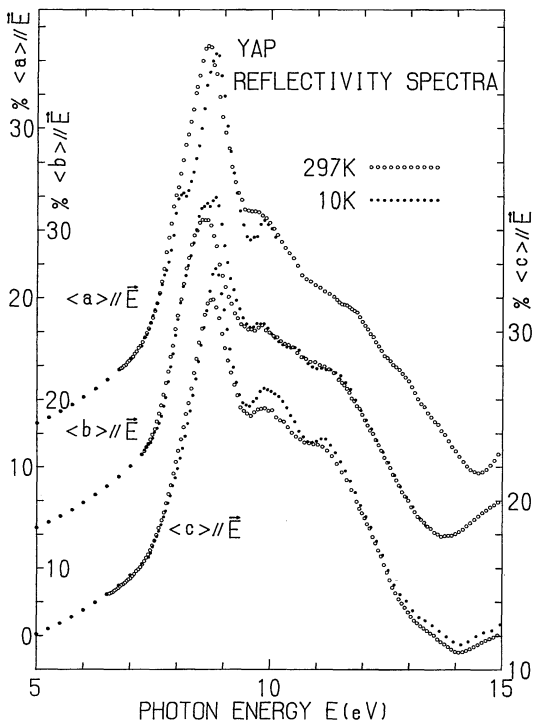

Fig. 4. Reflectivity spectra of YAP at 297 K (open circles) and 10 K (dots) which display temperature dependence in the range from 5 eV to 15 eV for $\langle a\rangle // E$, $\langle b\rangle // E$ and $\langle c\rangle // E$. Dots in the region of $E \lesssim 7$ eV stand for the reflectivity calculated from the refractive indices of eq. (3).

Table II. Energy positions (in eV) of structures observed in reflectivity spectra of YAP for $\langle a\rangle // E$; p, s, ws and [ ] stand for peak, shoulder, weak shoulder and uncertain, respectively.

R for $\langle a\rangle // E$ [eV]			R for $\langle a\rangle // E$ [eV]			R for $\langle a\rangle // E$ [eV]		
297 K			10 K			297 K		
8.010±0.05	s		8.119	p		78.51±0.03	s	
8.647	p		8.810	p		78.97	p	
9.664±0.075	s		9.859	p				
10.35 ±0.05	[ws]					80.2 ±0.15	s	
11.15 ±0.10	s					82.0 ±0.2	s	
11.58 ±0.06	ws					84.7 ±0.2	ws	
12.7 ±0.1	ws					86.89	p	
13.4 ±0.1	ws					89.7 ±0.2	s	
15.28 ±0.10	ws		15.28 ±0.10	ws		95.6 ±0.3	ws	
16.28 ±0.10	s		16.28 ±0.10	s		99.0	p	
18.18	p		18.18	p		101.1 ±0.3	ws	
18.89 ±0.16	s		18.89 ±0.16	s		109 ±1.5	ws	
21.66 ±0.36	s		21.66 ±0.36	s				
25.16 ±0.25	s							
27.98 ±0.30	s							
30.55 ±0.30	s							
32.05 ±0.30	s							
34.75	p							
36.25 ±0.30	ws							
37.45 ±0.30	s							
40.1 ±0.3	[s]							
47.65 ±0.5	ws							

Table III. Energy positions (in eV) of structures observed in reflectivity spectra of YAP for $\langle b\rangle // E$; p, s, ws and [ ] stand for peak, shoulder, weak shoulder and uncertain, respectively.

R for $\langle b\rangle // E$ [eV]			R for $\langle b\rangle // E$ [eV]			R for $\langle b\rangle // E$ [eV]		
297 K			10 K			297 K		
8.15 ±0.05	s		8.226±0.05	s		78.55±0.03	s	
			8.567±0.05	s		78.97	p	
8.586±0.05	p		8.810	p				
9.74 ±0.08	p		9.781	p		80.3 ±0.1	s	
10.31 ±0.08	s		10.53	s		81.5 ±0.2	s	
10.95 ±0.1	s		11.19 ±0.1	s		84.5 ±0.2	s	
12.15 ±0.05	s		12.10 ±0.05	s		86.69±0.05	p	
15.19 ±0.1	s					89.6 ±0.3	s	
16.7 ±0.1	s					97.3 ±0.4	s	
17.98 ±0.06	p					99.30	p	
18.6 ±0.1	ws							
20.25 ±0.2	ws							
21.3 ±0.2	ws							
22.65 ±0.2	ws							
25.94	p							
30.40 ±0.15	s							
32.05 ±0.3	s							
34.45	p							
37.45 ±0.3	ws							
40.5 ±0.5	[ws]							
47.4 ±0.7	ws							

structure. The shoulder at ~8.2 eV and three shoulders in the region from 9.5 eV to 12 eV are discernible more distinctly at 10 K. The low-energy peak for $\langle c\rangle // E$ shifts, with decreasing temperature, from ~8.74 eV at 297 K to 8.810 eV at 10 K; at the same time the line shape becomes sharper slightly. Subsequent two structures are recorded more distinctly at ~9.9 eV and ~11.2 eV at 10 K.

The spectra of YAP in the energy region $E \gtrsim 76$ eV are shown on expanded scales in Fig. 5 for $\langle a\rangle //$, $\langle b\rangle //$ and $\langle c\rangle // E$. The lowest-energy sharp line measured with each polarized light has a shoulder at ~78.5 eV on the lower energy side of the peak at ~79 eV, the energy separation being ~0.45 eV (cf. Tables II–IV). The doublet structure arises from the L_2 and L_3 levels of Al^{3+} which result from the spin-orbit interaction in the L-levels, L_2 being deeper. As shown in Fig. 2, the doublet lines split most distinctly for α-Al_2O_3 with an energy separation of 0.44 eV for $\langle c\rangle // E$[8] which is in almost agreement with the above

Table IV. Energy position (in eV) of structures observed in reflectivity spectra of YAP for $\langle c\rangle // E$; p, s, ws and [ ] stand for peak, shoulder, weak shoulder and uncertain, respectively.

R for $\langle c\rangle // E$ [eV]			R for $\langle c\rangle // E$ [eV]			R for $\langle c\rangle // E$ [eV]		
297 K			10 K			297 K		
8.14 +0.05	ws		8.23 +0.05	ws		78.54+0.03	s	
8.739+0.03	p		8.810	p		78.96+0.01	p	
9.883	p		9.937+0.07	p				
10.92 +0.10	s		11.20	p		80.3 +0.2	s	
13.32 +0.15	s		13.35+0.15	s		81.6 +0.2	s	
15.19	p					84.6 +0.2	ws	
17.93	p					86.89	p	
18.73 +0.15	s					89.9 +0.4	s	
21.29	s					96.1 +0.2	s	
24.2 +0.2	ws					99.91+0.2	p	
25.7 +0.3	ws					102.6 +0.4	ws	
30.55 +0.3	s					110 +1.5	s	
32.35 +0.3	ws							
34.75	p							
38.05 +0.3	ws							
42.85 +0.3	[s]							
49.15 +0.6	ws							

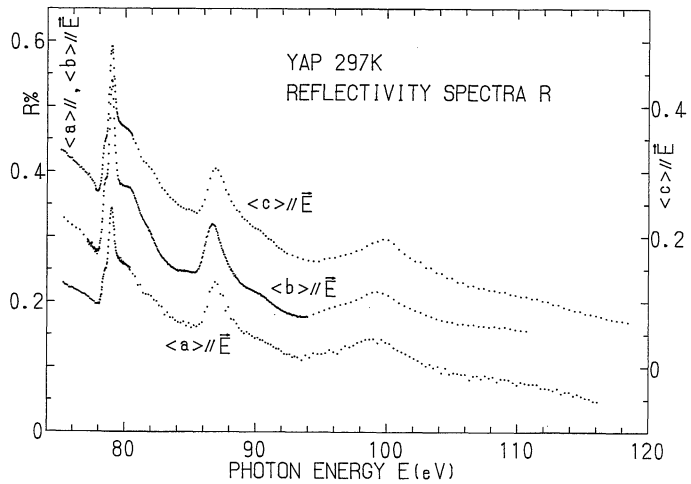

Fig. 5. Reflectivity spectra of YAP single crystals at 297 K for $\langle a\rangle // E$, $\langle b\rangle // E$ and $\langle c\rangle // E$ in the $Al^{3+}L_{2,3}$ region.

values.

The main features listed in Tables II–IV may be ascertained in the spectra in Fig. 5. One notices on Fig. 2 that the spectral behaviour in the region $E \gtrsim 76$ eV depends on the host lattice.

§4. Discussion

Our experiments permit the determination of relative values of the reflectivity. As shown in Fig. 1, absolute values of the reflectivity $R(E)$ (full curves) have been determined by normalizing the measured relative values to absolute values calculated from the refractive indices of eq. (3) (broken curves). It has been noticed to be essential, in achieving the Kramers-Kronig (abbreviated as K.K.) analysis of the reflectivity spectrum, that the reflectivity spectrum should be as free as possible from two kinds of errors: They are (i) errors introduced into the photon-energy dependence of the reflectivity and (ii) errors in the absolute magnitudes of the reflectivity spectrum. Discussion on accuracies of the present data is given in this section by describing difficulties encountered in the K.K. analysis and by applying the sum rule involving $\varepsilon_2(E)$ to the effective optical dielectric constant $\varepsilon_\infty(E)$, $\varepsilon_2(E)$ being the imaginary part of the dielectric function $\varepsilon(E)=\varepsilon_1(E)+i\varepsilon_2(E)$.

In order to define the reflectivity function over the entire region of $0 \leq E \leq \infty$ for the K.K. analysis, our reflectivity spectrum $R(E)$ measured in the region $E_L \leq E \leq E_M$ has been supplemented by the function

$$R(E)=R(E_M)\left(\frac{E}{E_M}\right)^{-p} \quad \text{for } E_M \leq E \leq \infty \tag{5}$$

and by the reflectivities calculated from the refractive indices of eq. (3) for $0 \leq E \leq E_L$. Here, E_M and E_L are the highest and lowest photon energies of the experimental region, respectively. The parameter p has been selected so that the absorption constant $A(E)=(4\pi E/ch)k(E)$ derived from $R(E)$ through the K.K. relations reasonably well conforms to the prediction by the Urbach rule. Here, $k(E)$ is defined by the complex index of refraction $\hat{n}(E)=n(E)+ik(E)$, and the Urbach rule for $A(E)$ of the absorption tail in the intrinsic region of YAP was given in I.

With the extension of E_M from ~ 40 eV to ~ 120 eV, but with E_L fixed at several eV, the K.K. analysis of reflectivity spectra becomes increasingly difficult to be performed: We have often met with such a reflectivity spectrum from which the K.K. relation could not derive the $A(E)$ compatiable with the Urbach rule for any positive value of p, or from which the K.K. relations could for certain value of p but the derived $A(E)$ changed sign to negative at energies above several 10 eV. This is admit-

tedly caused by errors (i) and/or (ii) involved in the reflectivity spectrum, because such a difficult situation in the K.K. analysis is avoidable with the reflectivity spectra measured under the criterion of eq. (1). One may readily understand that it will not be an easy task, in view of the K.K. relations, to find the absorption constants compatible with the Urbach

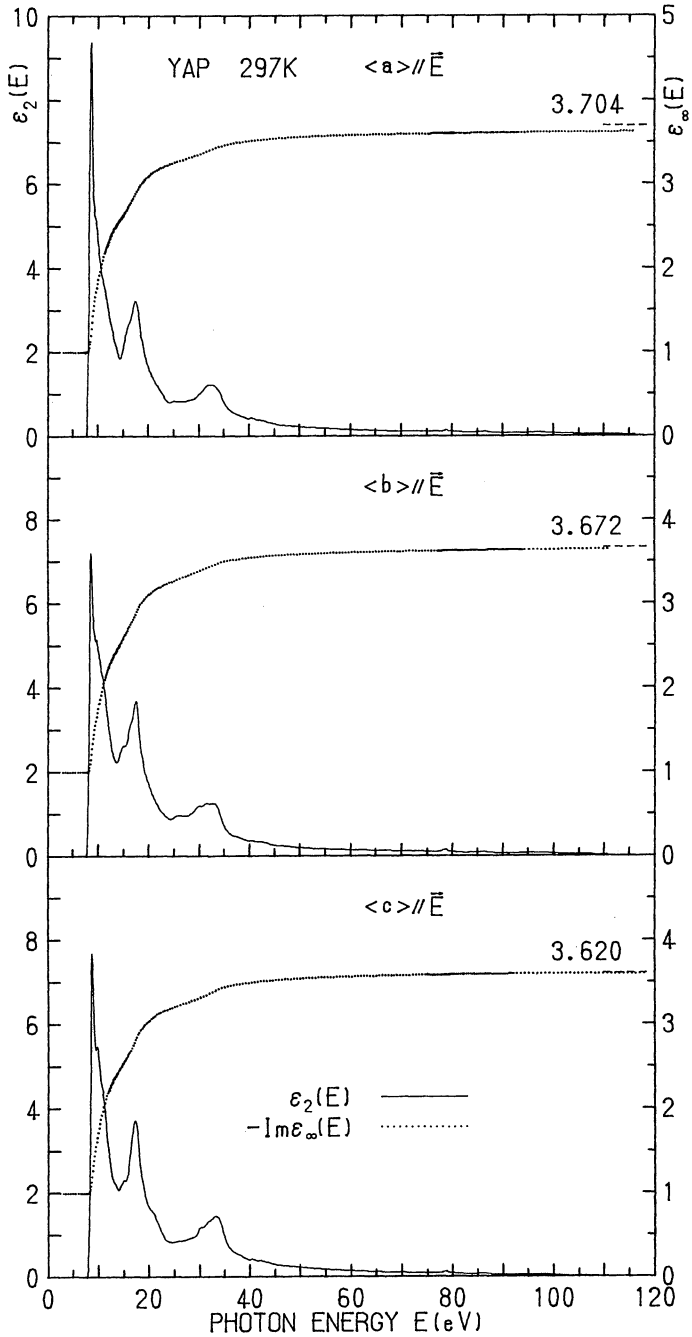

Fig. 6. A plot of $\varepsilon_\infty(E)$ vs E (dotted curve) for each of $\langle a\rangle /\!/ E$, $\langle b\rangle /\!/ E$ and $\langle c\rangle /\!/ E$. The spectra of $\varepsilon_2(E)$ used as the integrand of eq. (6) are shown by the full curves. The broken line segment stands for the optical dielectric constant $\varepsilon_{\infty,j}$ as indicated by the numeral for each of j=a, b and c (cf. eq. (4)).

rule in several eV region selecting the value of p in eq. (5) with $R(E_M) \sim 0.1\%$ at $E_M \sim 10^2$ eV. A reflectivity spectrum may be regarded as reliable if the spectrum has been obtained under the condition of eq. (1) and is transformed through the K.K. relations into optical constants acceptable from physical viewpoint over the entire region of $E_L \leq E \leq E_M$.

Estimate on the accuracy of the absolute magnitude of the reflectivity spectrum $R(E)$ measured under the condition of eq. (1)* may be obtained by the sum rule involving ε_2:[17]

$$\varepsilon_\infty(E) = 1 + \frac{2}{\pi}\int_0^E \frac{\varepsilon_2(E)}{E}\,dE. \qquad (6)$$

Here, use is made of $\varepsilon_2(E)$ which has been derived from the $R(E)$ in Fig. 1 through the K.K. analysis with the selection of an appropriate value of p in eq. (5). Our reflectivity function supplemented in the region of $0 \leq E \leq E_L$ contains no contribution from the lattice vibration (cf. eq. (3)). The infinite range of integration of eq. (6) is hence to lead $\varepsilon_\infty(E)$ to the optical dielectric constant ε_∞; $\varepsilon_\infty(E)$ is the effective optical dielectric constnat.

A plot of $\varepsilon_\infty(E)$ (dotted curve) and $\varepsilon_2(E)$ (full curve) as derived from our reflectivity spectrum in Fig. 1 is given as functions of E in Fig. 6 for $\langle a\rangle //$, $\langle b\rangle //$ and $\langle c\rangle // E$. The broken-line segment and numeral represent the value of $\varepsilon_{\infty,j}$ derived from the independent dispersion experiment, eq. (4); j=a, b and c. The dotted curve of $\varepsilon_\infty(E)$ for each frame of Fig. 6 is seen to saturate towards a value corresponding to $\varepsilon_{\infty,j}$ as E tends to E_M. Following values are obtained:

$$\left.\begin{aligned} \varepsilon_\infty(E_M) &= 3.62_9, \quad E_M = 116.1 \text{ eV for } \langle a\rangle // E \\ \varepsilon_\infty(E_M) &= 3.64_5, \quad E_M = 110.7 \text{ eV for } \langle b\rangle // E \\ \varepsilon_\infty(E_M) &= 3.60_7, \quad E_M = 118.4 \text{ eV for } \langle c\rangle // E \end{aligned}\right\}. \qquad (7)$$

$\varepsilon_{\infty,j}$ is the greatest in magnitude for j=a and diminishes in the alphabetic order as indicated by eq. (4). On the contrary, $\varepsilon_\infty(E_M)$ is estimated smaller for $\langle a\rangle // E$ than for $\langle b\rangle // E$ in eq. (7). In this respect, our $\varepsilon_\infty(E_M)$ is not fully in agreement with $\varepsilon_{\infty,j}$. In spite of this, one may notice $\varepsilon_\infty(E_M)/\varepsilon_{\infty,j} = 0.98_0$, 0.99_3 and 0.99_7 for $\langle a\rangle //$, $\langle b\rangle //$ and $\langle c\rangle // E$, respectively. Hence the reflectivity spectra in the present experiment are reliable within our experimental errors.

The present work has been performed under the approval of the Photon Factory Program Advisory Committee, Proposal No. 86-070 and No. 88-191.

* Otherwise, eq. (6) does not always guarantee the absolute magnitude, *e.g.*, cf. ref. 9.

References

1) M. J. Weber, M. Bass, K. Andringa, R. R. Monchamp and E. Comperchio: Appl. Phys. Lett. **15** (1969) 342.
2) K. W. Martin and L. G. DeShazer: Appl. Optics **12** (1973) 941.
3) M. J. Weber: J. Appl. Phys. **44** (1973) 3205.
4) V. N. Abramov and A. I. Kuznetsov: Sov. Phys.-Solid State **20** (1978) 399.
5) T. Tomiki, F. Fukudome, M. Kaminao, M. Fujisawa and Y. Tanahara: J. Phys. Soc. Jpn. **55** (1986) 2090.
6) T. Tomiki, F. Fukudome, M. Kaminao, M. Fujisawa, Y. Tanahara and T. Futemma: J. Lumin. **40 & 41** (1988) 379.
7) T. Tomiki, M. Kaminao, Y. Tanahara, T. Futemma, M. Fujisawa and F. Fukudome: J. Phys. Soc. Jpn. **60** (1991) 1799.
8) T. Tomiki, Y. Ganaha, T. Shikenbaru, T. Futemma, M. Yuri, Y. Aiura, S. Sato, H. Fukutani, H. Kato, T. Miyahara, A. Yonesu and J. Tamashiro: J. Phys. Soc. Jpn. **62** (1993) 573.
9) T. Tomiki, T. Shikenbaru, Y. Ganaha, T. Futemma, H. Kato, M. Yuri, H. Fukutani, T. Miyahara, S. Shin, M. Ishigame and J. Tamashiro: J. Phys. Soc. Jpn. **61** (1992) 2951.
10) T. Tomiki, Y. Ganaha, T. Shikenbaru, T. Futemma, M. Yuri, Y. Aiura, H. Fukutani, H. Kato, J. Tamashiro, T. Miyahara and A. Yonesu: J. Phys. Soc. Jpn. **62** (1993) 1388.
11) J. Reader, Gabriel L. Epstein and J. O. Ekberg: J. Opt. Soc. Am. **62** (1972) 273.
12) T. Tomiki, J. Tamashiro, Y. Tanahara, A. Yamada, H. Fukutani, T. Miyahara, H. Kato, S. Shin and M. Ishigame: J. Phys. Soc. Jpn. **55** (1986) 4543.
13) T. Tomiki, F. Fukudome, M. Kaminao, M. Fujisawa, Y. Tanahara and T. Futemma: J. Phys. Soc. Jpn. **58** (1989) 1801.
14) T. Tomiki, Y. Ganaha, T. Futemma, T. Shikenbaru, Y. Aiura, M. Yuri, S. Sato, H. Fukutani, H. Kato, T. Miyahara, J. Tamashiro and A. Yonesu: J. Phys. Soc. Jpn. **62** (1993) 1372.
15) T. Tomiki, T. Futemma, H. Kato, T. Miyahara, Y. Aiura, H. Fukutani and T. Shikenbaru: J. Phys. Soc. Jpn. **58** (1989) 1486.
16) J. A. Bearden and A. F. Burr: Revs. Mod. Phys. **39** (1967) 125.
17) H. R. Phillip and H. Ehrenreich: Phys. Rev. **129** (1963) 1550.